PHYSICAL REVIEW B VOLUME 27, NUMBER 4 15 FEBRUARY 1983

Electronic structure of Ni and Pd alloys. II. X-ray photoelectron core-level spectra

F. Ulrich Hillebrecht, John C. Fuggle, Peter A. Bennett,* and Zygmunt Zołnierek†
Institut für Festkörperforschung der Kernforschungsanlage Jülich,
D-5170 Jülich, Federal Republic of Germany

Ch. Freiburg
Zentralinstitut für Chemische Analysen der Kernforschungsanlage Jülich,
D-5170 Jülich, Federal Republic of Germany

(Received 11 May 1982)

Our measurements of the Ni 2*p* core levels in about 30 alloys show a dependence of the satellite on the chemical environment, which for a given stoichiometry correlates with the electronegativity of the partner. In no case was a complete disappearance of the satellite observed, which is interpreted as evidence for *d* character in unoccupied states. The general view developed in the preceding paper, that despite the band filling there is no large charge transfer in Ni intermetallic compounds, is confirmed by these observations. The band filling is a result of the mixing of wave functions which are centered on different sites. Studies of the satellite intensity as a function of stoichiometry in alloys with electropositive metals show the satellite to weaken as long as the band is being filled, and then to reach an almost constant intensity at some partner-element concentration. It is not possible to extract similar information from the spectra of Pd compounds because the satellites are weaker and partially obscured by inelastic losses.

I. INTRODUCTION

The preceding paper,[1] hereafter referred to as paper I, discussed the x-ray photoelectron (XPS) valence-band spectra of about 60 Ni and Pd alloys. Evidence in that paper indicated that the Ni and Pd *d* bands were more full in alloys with electropositive elements. It was argued that information on charge-transfer effects was not directly available from valence-band spectra, but the calculations indicated that the charge transfer was not large. The purpose of this paper is to discuss the possibility that such information can, in principle, be obtained from XPS core-level line shapes, particularly for Ni alloys, and to present a data basis for such work. We will discuss the origin of core-level satellites in Ni and Pd alloys and show a strong dependence on chemical environment, whereby trends in intensity and position parallel some trends in simple parameters, such as partner electronegativity. The concept of band filling will give the basis for the discussion of the role of the satellite.

Satellites and peak asymmetry arise in core-level XPS spectra because the potential felt by the valence electrons in the final state is not the same as that in the initial state. This change in potential changes the wave functions in the final states so that transitions from the initial state Ψ_i to more than one final state Ψ_f^n are allowed with a probability p given by[2–6]

$$p = |\langle \Psi_f^n | \Psi_i \rangle|^2 . \quad (1)$$

Evaluation of the matrix elements and Ψ_f^n in (1) is not a trivial problem, but the studies of Ni (Refs. 7–15) allow us to give a simple picture of the physics behind the satellites. Figure 1 gives a simplified scheme for interpretation of the Ni spectra. In this scheme the ground-state configuration of Ni is written as a linear combination of atomlike Ni d^9 and Ni d^{10} wave functions,

$$\Psi = a\Phi(d^9) + b\Phi(d^{10}) . \quad (2)$$

The $\Phi(d^n)$ include the appropriate s electrons and must be nearly degenerate in the ground state of the solid because with 9.4 electrons in the Ni d band[16–19] both configurations contribute to the ground state. In the presence of a core hole the two configurations are no longer degenerate so that two peaks are observed in the spectrum about 6 eV apart, as shown in Fig. 1.

A scheme as simple as that in Fig. 1 generates the hope that one may use the Ni-satellite intensities as

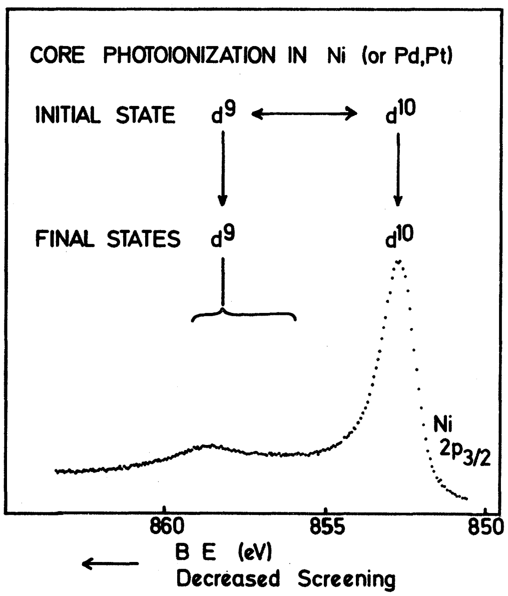

FIG. 1. Schematic diagram of interpretation of Ni $2p_{3/2}$ XPS spectrum. The $2p^5 3d^9$ final state has multiplet splitting.

a measure of the number of holes in the *d* band[15] because, other things being equal, the satellite intensity would increase as the weight of the d^9 configuration in the ground state increases. However, several complexities must be treated before this hope can be realized. The labels d^9 and d^{10} used in Eq. (2) neglect hybridization effects which reduce the *d* count in Ni to 8.8 electrons per atom and should be included in a description of the $\Phi_i(d^n)$.[23] In a scheme like the one outlined here one should also consider configuration interaction in the final states

$$\Psi_f(d^n)=a\Phi_f(d^9)+b\Phi_f(d^{10}) .$$

A clue to the degree of hybrization in the final states is available if we say that the change in potential of the valence electrons due to a deep core hole in element *Z* is similar to that due to an extra nuclear charge. In this "$Z+1$ approximation"[20–22] the core-ionized Ni atom looks like a Cu atom, and in Cu hybridization between *s* and *d* bands reduces the *d* count from 10 to approximately 9.6.[23] It can be seen from these arguments that hybridization severely affects quantitative interpretation of the core-level spectra of Ni and its compounds. Nevertheless despite the approximations involved, the labels attached to the features in Fig. 1 can be justified. For instance multiplet structure has been observed in core-level XPS satellites arising from the interaction of the core holes with the local $3d^9$ configuration.[13,24,25]

Because of the complications involved, the above scheme is at present more suitable for qualitative explanation of the spectra than quantitative treatment of the influence of the number of *d* holes. There are other schemes tied more or less to the concept of a screening orbital.[15,26–36] In a metal a core hole is screened by an increased concentration of valence electrons near the core hole. In metals such as Ni or rare earths the energetically most favorable distribution of this screening charge corresponds to an almost atomlike orbital. In many descriptions[26–30] the screening orbital is considered to be centered above the Fermi level in the initial state, and to be pulled below E_F in the final state. The probability of occupation of the screening orbital depends on its coupling to the rest of the valence electrons and its degree of occupation in the initial and final states. If the screening orbital is strongly localized, and its occupation in the initial state is low then the probability of its occupation in the final state is low and the screening cloud will have a radial distribution more like that of the other valence electrons. In the case of Ni $2p$ ionization this would correspond to a $2p^5 3d^9$ final state, where the $4s$ electrons take over the role of screening. Excitation may also take place to other final states where the screening cloud is still further from the core hole. Excitations to these more energetic final states contribute to the high-binding-energy (BE) tail of the peaks.

Not all of the screening schemes are appropriate for treating the dynamics of photoemission from Ni and the observed line shapes. In Ni the so-called screening orbital has no existence as a single orbital in the ground state, but is spread throughout the unoccupied bands. The original Toyozawa and Kotani[26,27] and Schönhammer and Gunnarsson[28,29] schemes apparently do not take the band character of the ground state sufficiently into account to treat core-level line shapes and the dynamics of photoemission from Ni. (We are not implying they are poor models: they were designed for different systems.) These models predict that the probability of screening orbital occupation in the final state depends on its position in the initial state. If the initial state position is closer to E_F then the probability of its occupation is higher and most of the XPS intensity is found in the "well-screened" peak at low BE. This clearly does not fit the case of Ni where there is a high density of unoccupied states just above E_F leading to intense satellites.

Kotani's calculations[27] included the influence of hybridization between the band of screening orbitals and the other bands of the system. That calculation (Fig. 5 in Ref. 27) showed that as the width of the hybridized "screening orbital" was increased the satellite intensity decreased.

The treatment of Penn[31] for valence band and of Tersoff, Falicov, and Penn[37] for core-level XPS is apparently also appropriate for reproducing the behavior found in experiment. They use a t-matrix approximation to calculate the scattering of the valence electrons from the potential of a valence band (VB) or core hole. In Ni there is a high density of states (DOS) above E_F so that there are many final states into which the electrons can scatter. A reduction of the DOS at E_F leads to weaker satellites because there are fewer final states into which the electrons can scatter. Furthermore it is concluded that the contribution of empty *sp* bands to a satellite is weak because a scattering of d electrons into *sp* states has low probability.

We may summarize the lessons of the calculations on the distribution of intensity in the core-level XPS spectra[27,31–33] as follows. Unoccupied Ni d character above E_F in Ni and its compounds can contribute to final states with a $3d$ hole at the core-ionized site (d^9 final states). The intensity of the satellite is determined by the weight of unoccupied Ni $3d$ character *and* by its position above E_F. Ni $3d$ character far above E_F produces a smaller contribution to the d^9 satellites than d character just above E_F. The model of Ni d character distribution drawn in paper I emphasized that there were ~ 0.6 holes in the Ni d band just above E_F, and approximately 0.6 $3d$ holes per atom distributed in the Ni *sp* bands at higher energy. Although no numerical calculations have been done, we will argue on the basis of the present data, that the holes in the Ni $3d$ band give the dominant contribution to the core-level satellite. However, in intermetallic alloys with electropositive metals the Ni $3d$ band is filled and the contribution due to unoccupied Ni $3d$ character in other bands becomes more important.

Pd is in the same group of the periodic system as Ni, and also has a nearly filled d band. The average number of electrons in the valence band is 9.6 electrons per site.[23] However, the $4d^9$ satellite in Pd and Pd alloys is weaker than in Ni and its alloys. Furthermore, electron-energy-loss measurements reported here reveal that in pure Pd and several of its alloys there is a strong extrinsic loss occurring at the same energy where in XPS the satellite appears. This makes an analysis similar to Ni and Ni alloys impossible.

Another aspect is the shape of the core lines. In general the shape of a core line is asymmetric. This is due to excitations of electron-hole pairs at the Fermi edge.[38,39] Different degrees of asymmetry can be understood very easily: The creation of an electron-hole pair is more probable if there are more occupied and unoccupied states close to the Fermi level. The asymmetry therefore contains information about the DOS close to E_F. This can be correlated with VB spectra. By comparing the asymmetries of core lines from different components of an alloy one can hope to be able to characterize the nature of the states close to E_F.

A fact which makes the analysis of the line asymmetry difficult if not impossible is that there may be multiplet splitting. In Ni the fully screened final state has a d^{10} configuration, therefore we do not expect a multiplet splitting. The satellite corresponds to a $2p^5 3d^9$ configuration, which has a multiplet structure. Some of its components are very close to the d^{10}-emission line, which affects its shape.[13] For this reason we have not performed a detailed line-shape analysis on the spectra presented in this paper although we discuss qualitative trends.

The last parameters from core-level XPS which might give information on the ground-state electronic structure are the core-level shifts and satellite energies. In many compounds XPS core-level chemical shifts can be related to the charge transfer between the atoms.[5,40] However, in intermetallic compounds, the charge transfer is smaller so the contribution to the shifts from this source is smaller. Also the core-level shifts seem to correlate strongly with the thermodynamic contribution due to dissolving a $Z+1$ atom in the host matrix[21,41,42] which introduces a new factor into the problem. We will restrict ourselves here to details of the core-level shifts relating to changes in the ground-state d count in alloys.

II. EXPERIMENTAL

Sample preparation, characterization, crystal structures, and details concerning the XPS measurements have been described in Sec. III paper I. In this paper we also present some electron-energy-loss measurements (ELS), which were performed in the XPS machine in the reflection mode. We used a Vacuum Generators LEG 22 electron gun, and the same analyzer as for XPS. The primary energy was 1500 eV. The angle between the incident electron beam and the direction of detection was about 60°, but we did not use specular geometry. The ELS spectra were not strongly dependent on geometry as long as no grazing angles were used. As for XPS measurements, the samples were cleaned by scraping with an aluminium oxide file. Contamination was controlled by XPS before and after the ELS measurements. It was not larger than that quoted for our XPS results—up to 3 at. %—as the time required for one spectrum was at the most 1 h.

III. RESULTS AND INTERPRETATION

A. XPS and ELS on Pd alloys

For the discussion of core-level spectra which exhibit satellites it is first of all important to establish the nature of these satellites. Whereas in Ni it is unambiguously proven that the satellite is intrinsic,[25,43] we think the situation is not so clear in Pd. Chandesris *et al.*[44] found a resonant enhancement of the satellite at 53-eV photon energy, which supports an interpretation of the satellite as being—maybe partially—intrinsic. However, energy-loss measurements with 60-keV electrons in transmission[45] and with 0.2- to 0.8-keV electrons in reflection[46] show a peak at 7.4-eV energy loss. The satellite in XPS occurs at ~6.5 eV higher BE than the main line, therefore it may be affected by an extrinsic loss at 7.4 eV. Mårtensson *et al.*[47] measured Cu-Pd alloys and, because with the Cu $2p_{3/2}$ line there was no satellite at the same energy as with the Pd lines, they concluded that the Pd satellite was largely intrinsic in those alloys. In the following we will show that the extrinsic satellite contribution varies between Pd and its alloys, and that it is not always possible to ignore it as Mårtensson *et al.* could for Cu-Pd alloys. For this purpose it is necessary to discuss the significance of ELS spectra for XPS measurements. In our ELS experiments, the electrons reaching the detector had undergone a nonspecular scattering of about 60°. This large-angle scattering is mainly elastic. The angle associated with the inelastic scattering is small, because the inelastic cross section decreases with the second power of the scattering angle.[48] The primary energy of the impinging electrons was 1500 eV, so that the inelastic cross section is very similar to that for photoelectrons from the Pd $3d$ levels excited with Al $K\alpha$ radiation. With the exception that in the ELS measurement the electrons are passing the surface twice the ELS curve should give a good indication of the extrinsic loss function relevant for photoelectrons.

Figure 2 shows the ELS spectra obtained in the reflection mode for Pd, V_3Pd, $LaPd_3$, and La_7Pd_3. In Pd, we find a peak at 7.2-eV energy loss. The features in the V_3Pd spectrum are much less pronounced; a very flat maximum occurs at 10.5±0.5 eV. At higher energy losses the spectrum is essentially flat. The ELS spectrum for $LaPd_3$ has a maximum at 10.5±0.3 eV. In La_7Pd_3 we find a fairly pronounced peak at 12.4 eV. We note that the four ELS spectra shown in Fig. 2 are distinctly different.

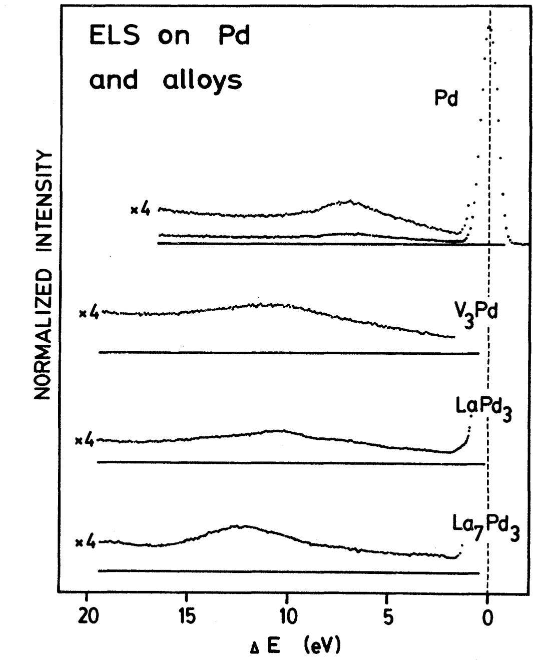

FIG. 2. Electron-energy-loss spectra obtained in the reflection mode at 1500-eV primary energy for Pd and three alloys, normalized to constant area of elastic peak as shown for Pd. Instrumental effects broadened the V_3Pd spectrum.

To assess the influence of the extrinsic losses on the XPS spectrum in the region of the satellites we used the ELS spectra shown in Fig. 2 for background subtraction. We employed the following procedure: We normalized the ELS spectrum so that the area of the elastic peak was equal to the area of the Pd $3d_{5/2}$ line. To this curve we added a second ELS curve shifted to lower kinetic energy by 5.3 eV, which is the spin-orbit splitting of the Pd $3d$ lines, and multiplied by $\frac{2}{3}$ to account for the lower intensity of the Pd $3d_{3/2}$ line. The curve obtained in this way represents the total extrinsic losses of the Pd $3d$ doublet. To obtain the intrinsic satellites, we subtracted this sum of two ELS spectra from the XPS spectrum. The result for Pd, V_3Pd, $LaPd_3$, and La_7Pd_3 is shown in Fig. 3. Naturally, the intensity of the satellite is reduced. In Pd the peak of the $3d_{3/2}$ satellite is shifted by 0.3 eV towards the

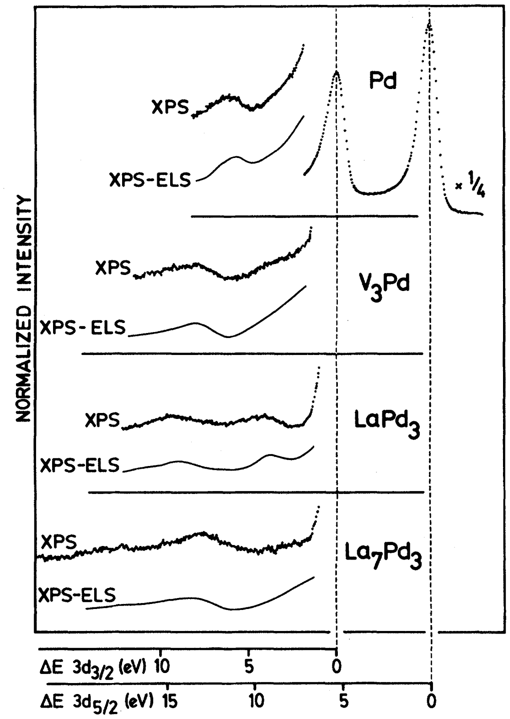

FIG. 3. Experimental spectra of Pd $3d$ doublets with satellites (dotted lines) and satellite region after subtraction of extrinsic losses (solid lines) for Pd and three alloys. For clarity the main peaks of the alloys' XPS spectra are not shown. The subtraction is described in the text. The two BE scales give the difference in BE with respect to the $3d_{3/2}$ and $3d_{5/2}$ lines.

main line, so that after the subtraction we find an intrinsic satellite separation of 5.8 eV as compared to 6.1 eV from the uncorrected XPS spectrum. In V_3Pd the loss function is fairly flat and the position of the satellite is not shifted by the subtraction. But the steady rise of the loss function up to approximately 11 eV leads to a large reduction of intensity about 10 eV below the $3d_{5/2}$ line and below.

A much more drastic example of distortion of the spectra by extrinsic losses occurs in La-Pd alloys (and also in alloys of Sc, Y, and the light rare earths with Pd). In the XPS spectrum of La_7Pd_3 there is a peak at 12.9 eV below the $3d_{5/2}$ line, and there is also a steplike feature at 12.5 eV below the $3d_{3/2}$ line. After subtracting the extrinsic losses we find a curve much more similar to Pd, where the peak at 13.5 eV below the $3d_{5/2}$ line now can unambiguously be assigned to an 8.2-eV satellite of the $3d_{3/2}$ line. The $3d_{5/2}$ satellite is—as in Pd—under the $3d_{3/2}$ main line. The similarity of the corrected XPS spectrum from La_7Pd_3 to the Pd XPS spectrum, and the satellite separation of 8.2 eV gives us confidence in the background subtracting procedure we used, because a satellite shift of 6 eV and an intensity as high as in the uncorrected XPS spectrum would have been in strong contrast to our results on Ni alloys described in Sec. IV *B*.

The evidence presented here shows that the extraction of information on intrinsic Pd XPS satellites is complicated by two factors. Firstly, there is the overlap of the $3d_{5/2}$ satellite with the $3d_{3/2}$ main line; secondly, the extrinsic losses contribute appreciably to the satellite and have to be removed from experimental XPS spectra. The overlap can be avoided by using a different core level, e.g., the $3p_{3/2}$ line, at the cost of an extra 2-eV width of the primary line. But in contrast to Ni, the intrinsic part in Pd alloys is not the predominant contribution to the satellite compared to the extrinsic part. We did not think it justified to measure the loss spectrum for each alloy in order to determine satellite characteristics because the uncertainties involved are nearly as large as the rather weak satellites. We would only like to state qualitatively that in cases where the loss spectrum does not have any pronounced influence on satellite position, shape, and intensity, like the V-Pd alloy series, the effect caused by alloying is qualitatively similar to what we observe in Ni. The satellite intensity decreases and its separation from the main line increases with increasing dilution of Pd in electropositive elements until at some partner element concentration a saturation is reached.

The $Z+1$ approximation for the treatment of final-state effects has been applied successfully to dilute alloys.[41,42] For a dilute alloy of an element Z in a host A one expects to find a large chemical shift of the levels of the Z element if the heats of solution of the Z and the $Z+1$ elements in A are very different. For nondilute alloys the argument should still be roughly valid, if the ternary term $E(Z+1;AB)$, which describes the energy of solution of a $Z+1$ atom in an A_xB_{1-x} alloy, is replaced by the weighted average $xE(Z+1;A)+(1-x)(Z+1;B)$ of the energies of solution of a $Z+1$ atom in the two components of the alloy. Tables I and II give the BE's of Pd core levels in Pd alloys, including the chemical shift averaged over the $3d$ levels. As an example to illustrate the predicted behavior we mention the Al-Pd alloys. According to Miedema *et al.*[49] the heat of formation for AlPd is $\Delta H = -84$ kJ/mole atom, whereas for AlAg, $\Delta H = -10$ kJ/mole atom. There is a large difference between these two heats of formation, and also the chemical shift of the Pd core lev-

TABLE I. BE's of Pd $3d_{5/2}$, $3d_{3/2}$, and $3p_{3/2}$ levels and satellities in Pd intermetallic compounds (in eV).

	BE[a] $3d_{5/2}$	ΔE_{sat}[b]	BE[a] $3d_{3/2}$	ΔE_{sat}[b]	BE[a] $3p_{3/2}$	ΔE_{sat}[b]	Chemical[c] shift
Pd	335.20	e	340.45	6.1 ± 0.4	532.3 ± 0.2	6.1 ± 0.4	
$Al_{0.1}Pd_{0.9}$	335.45	e	340.75	6.3 ± 0.5	532.5 ± 0.2	6.3 ± 0.5	0.3
AlPd	337.05[d]	e	342.35[d]	e	533.9 ± 0.3	e	1.9
Al_3Pd	337.70	e	342.90	e	534.6 ± 0.3	e	2.5
ScPd	336.35	8.4 ± 0.9	341.65	9.2 ± 0.6	533.3 ± 0.3	9.9 ± 0.5	1.2
$TiPd_3$	335.80	8.1 ± 1.0	341.05	7.7 ± 0.4	532.8 ± 0.2	f	0.6
VPd_3	335.60	e	340.90	7.2 ± 0.4	532.6 ± 0.3	7.4 ± 0.4	0.4
VPd_2	336.10	e	341.40	7.4 ± 0.4	533.2 ± 0.3	7.3 ± 0.4	0.9
VPd	336.10	e	341.40	7.9 ± 0.4	533.0 ± 0.3	7.8 ± 0.4	0.9
V_3Pd	336.50	e	341.75	8.1 ± 0.4	533.4 ± 0.4	8.7 ± 0.5	1.3
NiPd	335.65	e	340.90	6.7 ± 0.4	532.6 ± 0.3	f	0.5
$NbPd_2$	336.10	8.1 ± 0.8	341.40	7.9 ± 0.6	533.0 ± 0.3	8.2 ± 0.5	0.9
$TaPd_3$	336.00	8.5 ± 0.8	341.30	8.0 ± 0.6	533.0 ± 0.3	8.1 ± 0.5	0.8
$TaPd_2$	336.30	8.3 ± 0.6	341.60	8.2 ± 0.5	533.3 ± 0.3	8.1 ± 0.5	1.1
TaPd	336.50	8.5 ± 0.7	341.80	8.1 ± 0.5	533.4 ± 0.3	9.4 ± 0.7	1.3

[a] Uncertainty ± 0.2 eV unless otherwise stated.

[b] BE difference between main line and satellite; satellite has larger BE. Values taken from XPS spectra not corrected for extrinsic losses.

[c] BE (intermetallic compound) −BE (Pd), averaged over $3d$ levels.

[d] Uncertainty ± 0.3 eV.

[e] Overlap with other peaks.

[f] Not measured.

els is quite large. A complete analysis of the chemical shifts will be published separately.[50]

B. Ni alloys

For the following presentation of our results on Ni alloys we do not think it is necessary to show all experimental spectra. As the discussion of our results mainly concerns the satellites, we only select spectra which show certain effects important for determining satellite intensities or positions (or any other property of the satellites). Data not illustrated are shown in Tables III–V.

The intense core-level satellites in Ni are considered to be intrinsic.[9–15,42,43] We performed ELS measurements on some Ni alloys and found that also in the alloys the extrinsic contribution to the satellite was negligible compared to the intrinsic contribution. This justifies our procedure for calculating the satellite intensity from the experimental spectra (see appendix). The only exceptions from this rule are Al and Mg alloys with high Al or Mg concentrations. In Fig. 4 the Ni $2p_{3/2}$ photoemission spectra of Al-Ni alloys are shown. The main line becomes less asymmetric as the Al concentration increases. At the same time the satellite separation increases, at least in the case of $AlNi_3$

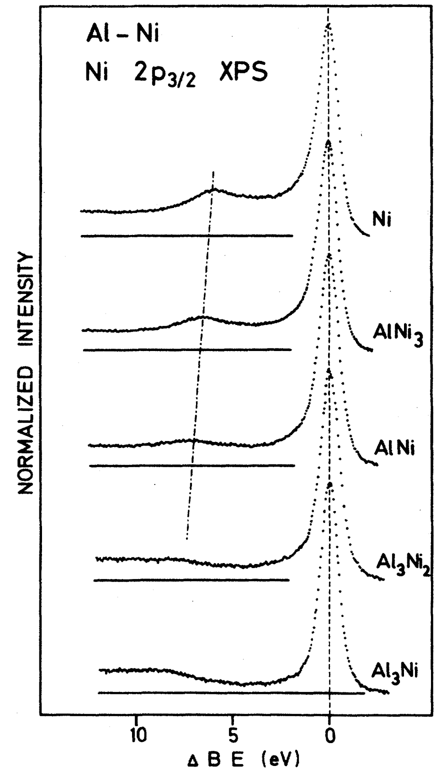

FIG. 4. Ni $2p_{3/2}$ XPS spectra from Al-Ni alloys, normalized to constant height of main peak.

TABLE II. Binding energies of Pd $3d_{5/2}$, $3d_{3/2}$, and $3p_{3/2}$ levels and satellites in Y, lanthanide, Th, and U intermetallic compounds with Pd (in eV).

	BE[a] $3d_{5/2}$	ΔE_{sat}[b]	BE[a] $3d_{3/2}$	ΔE_{sat}[b]	BE[a] $3p_{3/2}$	ΔE_{sat}[b]	Chemical[c] shift
Pd	335.20	d	340.45	6.1±0.4	532.3±0.2	6.1±0.4	
YPd_3	355.55	8.9±0.5	340.85	9.4±0.4	532.6±0.2	9.1±0.8	0.4
$LaPd_3$	335.75	9.5±0.5	341.05	9.2±0.5	532.9±0.3	9.4±0.6	0.6
$CePd_3$	335.85	9.2±0.5	341.15	9.2±0.5	532.8±0.3	9.4±0.6	0.7
$PrPd_3$	335.70	9.2±0.5	341.00	9.2±0.5	532.6±0.3	e	0.5
$NdPd_3$	335.80	9.0±0.5	341.05	9.4±0.5	532.9±0.3	e	0.6
$SmPd_3$	335.80	9.3±0.5	341.10	9.1±0.5	532.8±0.3	e	0.6
$ThPd_3$	336.25[d]	d	341.60[d]	e	533.0±0.4	f	1.0[f]
UPd_3	336.30		341.60	9.0±0.6	533.0±0.4	f	1.1
$LaPd_2$	336.10	e	341.35	e	533.1±0.3	10.3±0.5	0.9
Ce_3Pd_5	335.25	e	341.55	e	533.3±0.3	10.0±0.6	1.1
LaPd	336.40[g]	e	341.70[g]	e	533.3±0.3	10.6±0.8	1.2
CePd	336.20	9.1±1.0	341.50	e	533.3±0.3	9.9±0.5	1.0
ThPd	336.60[d,g]	d	f	d	533.6±0.3	f	1.4
Y_7Pd_3	336.75	13.3±0.5	342.00	12.5±0.8	533.8±0.3	11.6±1.0	1.6
La_7Pd_3	336.55	12.9±0.7	341.80	7.2±0.2	f	f	1.4
Ce_7Pd_3	336.60	e	341.90	e	533.7±0.3	10.9±0.7	1.4
Th_2Pd	336.70[d,g]	e	f	e	533.7±0.4	11.8±0.7	1.5
LaPdAl	336.60	e	341.90	e	533.6±0.3	12.8±0.8	1.4
CePdAl	336.55	e	341.80	e	533.6±0.3	e	1.4
ThPdAl	336.75	d		d	533.9±0.3	f	1.6

[a] Uncertainty ±0.2 eV unless otherwise stated.

[b] BE difference between main line and satellite; satellite has larger BE. Values taken from XPS spectra not corrected for extrinsic losses.

[c] BE (intermetallic compound) −BE (Pd), averaged over $3d$ levels.

[d] Overlap with other peaks.

[e] Too weak for reliable measurements.

[f] Not measured.

[g] Uncertainty ±0.4 eV.

and AlNi. The situation is not so clear with Al_3Ni_2 and Al_3Ni where the spectrum in the region of the satellite looks different from the other alloys. As the Al concentration in these two compounds is rather high, we interpret the flat region above 8-eV relative BE to be a plasmon. This is supported by comparison with Al $2s$ and $2p$ spectra from Al, Al_3Pd, and Al_3Ni in Fig. 5. In Al, the bulk plasmon is at 15.5 eV and the surface plasmon at 10.5 eV. In Al_3Pd, the bulk and surface plasmons are reduced and shifted, but clearly recognizable. In Al_3Ni, the plasmon loss of the Ni $3p$ levels is superimposed on the loss of the Al $2p$, leading to a plateau at 10 – 13.5 eV smaller kinetic energy. (The same problem occurs for the Al $2s$ level in Al_3Ni which overlaps with the Ni $3s$ loss structure.) The loss strength looks similar in Al_3Pd and Al_3Ni. We conclude that in Al_3Ni the Ni $2p$ lines are accompanied by a plasmon loss. This explains the plateau about 8 – 13 eV below the $2p_{3/2}$ line, and the tail of the $2p_{1/2}$ line to its low-BE side opposite to the Doniach-Šunjić losses.[9,39]

The strong extrinsic losses in Al_3Ni_2 and Al_3Ni make numbers for the intensity of the intrinsic Ni satellite less reliable but we believe weak satellites are still present in Al_3Ni_2 and Al_3Ni. For Al_3Ni_2 we draw this conclusion from a comparison with the Al_3Ni spectrum. The intensity in the Al_3Ni_2 spectrum in the region 3 – 5 eV below the main line, where the satellite contributes to the intensity, is higher than in the Al_3Ni spectrum. Furthermore, we have not observed a complete disappearance of the satellite in any of the alloys, so we think it is unlikely that the satellite should have disappeared in Al_3Ni. In Mg-Ni alloys plasmon losses also complicate the Mg_2Ni spectra.

We now come to alloys of the $4f$ and $5f$ series of the periodic system. The interpretation of spectra from La-Ni alloys is difficult because the Ni $2p_{3/2}$ and La $3d_{3/2}$ levels have almost identical BE's. For

TABLE III. Binding energies of Ni $2p_{1/2}$,$p_{3/2}$ levels and satellites in Ni intermetallic compounds (in eV).

	BE[a] $2p_{3/2}$	ΔE[b]	I_{sat}[c]	BE[a] $2p_{1/2}$	ΔE[b]	I_{sat}[c]	Chemical[d] shift	Electro[e] -negativity
Ni	852.65	5.80±0.4	29	869.90	4.60±0.4	28		1.8
$MgNi_2$	852.65	6.15±0.2	14	870.15	f		0.2	1.2
Mg_2Ni	852.70	6.60±0.4	14[g]	869.90	g	g	0.0	1.2
$AlNi_3$	852.65	6.55±0.2	21	869.95	5.00±0.4	25	0.0	1.5
AlNi	852.80	7.20±0.4	19	870.10[h]	5.65±0.4	23	0.20	1.5
Al_3Ni_2	853.40	8.00±0.6	12[g]	870.70[h]	6.65±0.4	12	0.75	1.5
Al_3Ni	853.75		10[g]	871.05		g	1.05	1.5
ScNi	852.80	6.95±0.4	27	869.85	5.75±0.4	25	0.05	1.3
TiNi	853.15	7.20±0.4	26	870.20	5.90±0.4	28	0.4	1.6
$CrNi_2$	852.95	6.35±0.4	26	870.15	4.90±0.3	26	0.3	1.6
CuNi	852.55	6.00±0.4	30	869.60	f		−0.2	1.9
PdNi	852.45	6.20±0.4	28	870.00	f		−0.05	2.0
InNi	852.35	6.70±0.3	20	869.55	5.45±0.5	25	−0.3	1.5
$TaNi_3$	852.75	6.85±0.3	22	869.95	5.35±0.4	27	0.1	1.5
$TaNi_2$	853.20	7.15±0.4	22	870.35	f		0.5	1.5
Ta_2Ni	853.30	7.10±0.3	21	870.55	5.45±0.4	19	0.65	1.5
AuNi	852.15	5.40±0.4	36	869.40	f		−0.5	2.3
UNi_5	852.90	6.80±0.4	24	870.10	5.30±0.4	24	0.2	1.6

[a] Uncertainty ±0.2 eV unless otherwise stated.

[b] BE difference between main line and satellite; satellite has larger BE.

[c] Satellite intensity as percent of total intensity of main line plus satellite. Uncertainty ±2%.

[d] BE (intermetallic compound) −BE (Ni), averaged over $2p$ lines.

[e] Electronegativity of partner element according to Ref. 57.

[f] Not measured or not observed.

[g] Obscured by plasmon loss.

[h] Uncertainty ±0.3 eV.

TABLE IV. Binding energies of the Ni $2p_{3/2}$ and Ni $2p_{1/2}$ levels and satellites in La_xNi, Ce_xNi, and Th_xNi intermetallic compounds (in eV).

	BE[a] $2p_{3/2}$	ΔE[b]	I_{sat}[c]	BE[a] $2p_{1/2}$	ΔE[b]	I_{sat}[c]	Chemical[d] shift
Ni	852.65	5.80±0.4	29	869.90	4.6±0.4	28	
$LaNi_5$[e]	852.65[f]	6.00±0.5	23[g]	869.80	4.6±0.5		−0.05
$CeNi_5$[e]	852.60	6.40±0.3	25	869.85	5.0±0.4	12	−0.05
$ThNi_5$[e]	852.80	6.45±0.3	23	870.10			0.20
$CeNi_2$	853.00	6.85±0.3	23	f			0.35
LaNi	f			870.10[h]	6.0±0.5	13	0.20
CeNi	853.00	6.90±0.3	20	870.10			0.30
ThNi	853.00	7.15±0.6	14	870.15			0.30
La_7Ni_3	f			869.95	6.8±0.8	12	0.05
Ce_7Ni_3	853.00	7.00±0.3	19	870.1			0.30
Th_7Ni_3	853.15	7.00±0.4	18	870.30	6.1±0.6	20	0.45
La_3Ni	f			869.90	5.0±0.4	10	0.00

[a] Uncertainty ±0.2 eV unless otherwise stated.

[b] BE difference between main line and satellite; satellite has larger BE.

[c] Satellite intensity in percent of total intensity of main line plus satellite.

[d] BE (intermetallic compound) −BE (Ni), averaged over $2p$ lines.

[e] Electronegativity of La and Ce:1.1,Th:1.2 (Ref. 57).

[f] Partially obscured by other peaks.

[g] Overlap with La $3d_{3/2}$ line, uncertainty ±4%.

[h] Uncertainty ±0.3 eV.

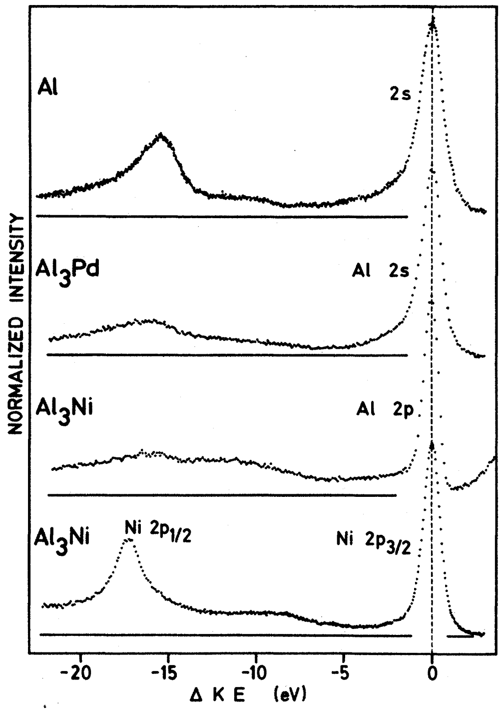

FIG. 5. Al $2s$ spectra from Al and Al_3Pd; Al $2p$ and Ni $2p$ spectra from Al_3Ni, normalized to constant height of largest peak. In the Al $2p$ spectrum from Al_3Ni the loss structure is a superposition of the Al $2p$ and the Ni $3p$ satellites. Note that Al $2s$ is narrower in Al_3Pd than in Al. Al $2s$ and part of Ni $2p$ were recorded with 0.05-eV stepwidth, the other spectra with 0.10-eV stepwidth.

this reason we consider the satellite of the $2p_{1/2}$ line. We see from Tables III and IV that the $2p_{1/2}$ satellite behaves in a similar way to the $2p_{3/2}$ satellite. Even here an estimate of the intensity of the $2p_{1/2}$ satellite in La-Ni compounds is not easy due to the La $M_{4,5}N_{4,5}N_{4,5}$ Auger transition with its peak at 630-eV kinetic energy. Because of the large width of the La MNN Auger decay all lines in this region have a background which for the Ni $2p_{1/2}$ slopes downwards with a negative curvature as the BE increases. Thus it is difficult to assess the satellite intensity even for the Ni $2p_{1/2}$ line, and the numbers given in Table III have a larger uncertainty of 4%. Nevertheless the effect of alloying La with Ni is quite large; in the 1:1 alloy the satellite contains only 13% of the intensity, the smallest fraction found for a 1:1 alloy.

The BE of the Ce $3d_{5/2}$ level is large enough so that there is no overlap with the Ni $2p_{3/2}$ line. Because the Ni $2p_{1/2}$ satellite at ~876-eV BE is affected by the Ce $3d_{5/2}$ line at ~882 eV we do not quote satellite intensities. In Fig. 6 the Ni $2p_{3/2}$ spectra of Ce-Ni alloys are shown. As in the Al-Ni and Ta-Ni systems the satellite intensity decreases and its separation from the main line increases. However, there is a saturation of these effects, because the position does not change between the 1:1 and 7:3 alloys; also the 1% difference in intensity is not significant.

The Ni $2p_{3/2}$ peaks from a series of Th-Ni alloys in Fig. 7 again show dramatic changes with increasing Th content. 17 at.% Th reduces the satellite intensity from 29 at.% in Ni to 23 at.% in $ThNi_5$, and the satellite is still less intense in ThNi. However, in Th_7Ni_3 it is stronger again and we note that its peak energy is closer to its main line than in ThNi. The Th-Ni alloy series is an example where we not only observe a saturation of the effect the alloying has on satellite position and intensity, but also at 70 at.% Th concentration a partial reversal of this effect.

In Fig. 8 we showed the Ni $2p_{3/2}$ spectra of alloys with the noble metals Cu and Au, and with Pd. The electronegativities of these metals are 1.9, 2.0, and 2.3, respectively, which is larger than the 1.8 for Ni.[51] The satellite intensity is not significantly changed in CuNi and PdNi, but in AuNi it is much larger than in Ni, namely 36%. The energy separation of the satellite decreases in the order CuNi, PdNi, then AuNi. An interesting feature which is

TABLE V. Binding energies of Ni $2s$, $3s$, and $3p$ levels in intermetallic compounds (in eV).

	$2s$	$3s$	$3p_{1/2}$	$3p_{3/2}$
Ni	1008.6±0.4		68.0±0.5	66.2±0.3
$AlNi_3$	1007.9±0.5		67.9±0.6	66.3±0.4
Al_3Ni_2		111.1±0.5	68.7±0.6	67.0±0.4
Al_3Ni	1008.3±0.8		69.0±0.6	67.3±0.4
ScNi			67.9±0.5	66.3±0.4
$LaNi_5$		110.6±0.3		
LaNi		110.8±0.4	68.2±0.7	66.6±0.5
Ce_7Ni_3			68.1±0.6	66.6±0.4
$TaNi_3$			67.9±0.6	66.3±0.4

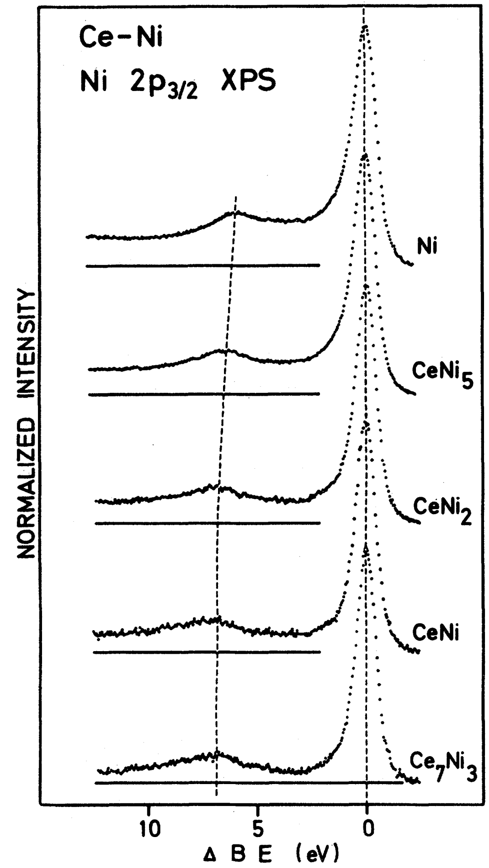

FIG. 6. Ni $2p_{3/2}$ XPS spectra from Ce-Ni alloys, normalized to constant peak height.

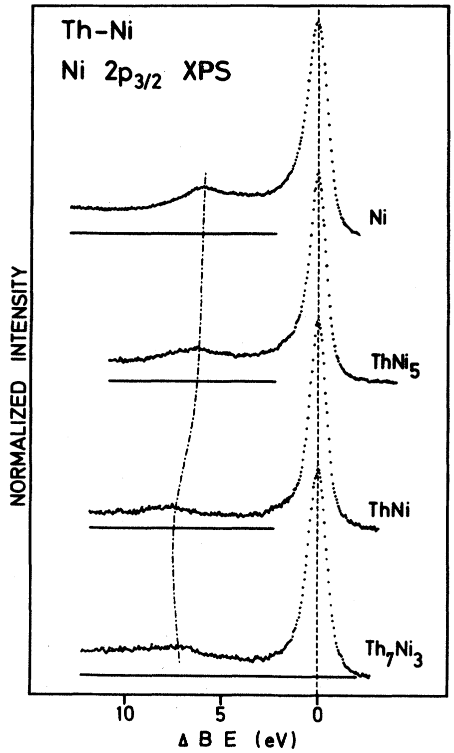

FIG. 7. Ni $2p_{3/2}$ XPS spectra from Th-Ni alloys, normalized to constant peak height.

shown by all spectra in Fig. 8 is an increased intensity between the main line and the satellite peak. This is probably due to the multiplet structure of the satellite as discussed later.

The AuNi result shows that it is possible to find a stronger satellite in an alloy than in Ni itself. An increased satellite has also been observed in Ni oxide[52] (and in NiF$_2$ and other transition-metal fluorides[7]).

IV. DISCUSSION

A. Satellite intensities

The general trends in satellite intensities are:

(1) In Ni compounds with a given electropositive element the satellite intensity tends to decrease with increasing dilution of the Ni, until at some dilution near 50% the effect saturates. Two examples are shown in Fig. 9.

(2) For a given stoichiometry the core-level satellites of Ni tend to decrease with partner electronegativity. This effect is shown for 1:1 compounds in Fig. 10.

The first observation can be rationalized in terms of the VB model from paper I which is reproduced in Fig. 11. This figure indicates that Ni has d character not only in the d bands close to E_F, but also in the Ni sp bands at higher energy. In alloys with electropositive metals the d band becomes filled, but unoccupied d character remains in the other bands, as shown by the calculations in paper I. The XPS spectra in paper I showed that the filling of the Ni d bands required typically 30 to 50 at. % of an electropositive partner element. Comparison of the data in Tables III and IV, or Fig. 9, with the XPS VB's in paper I shows that the Ni $2p$ satellite intensity always reaches its plateau value at the concentration where the density of the Ni $3d$ states at E_F falls nearly to zero. We thus assign the sharp decreases in Ni satellite intensity to the Ni $3d$-band-filling.

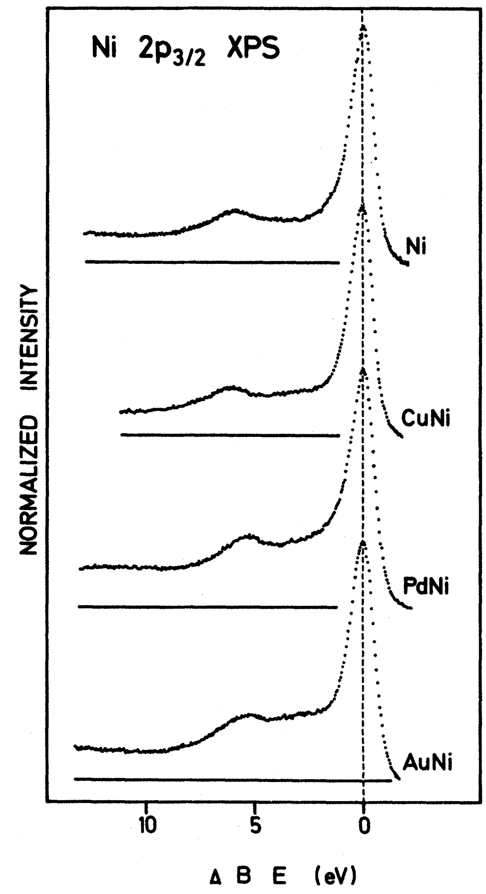

FIG. 8. Ni $2p_{3/2}$ XPS spectra from CuNi, PdNi, and AuNi, normalized to constant peak height.

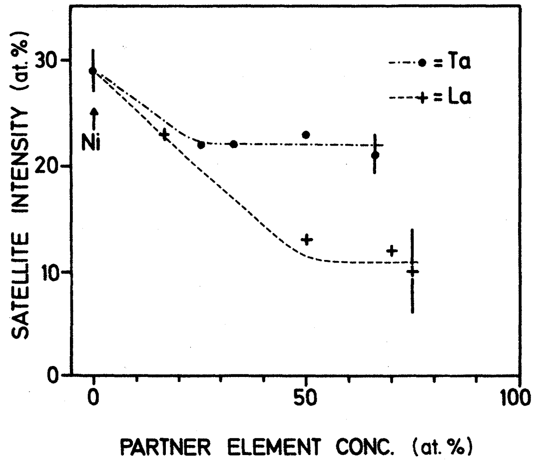

FIG. 9. Dependence of Ni $2p_{3/2}$ satellite intensity on concentration of partner element for Ta-Ni and La-Ni alloys. In Ni metal the satellite intensity is 29%.

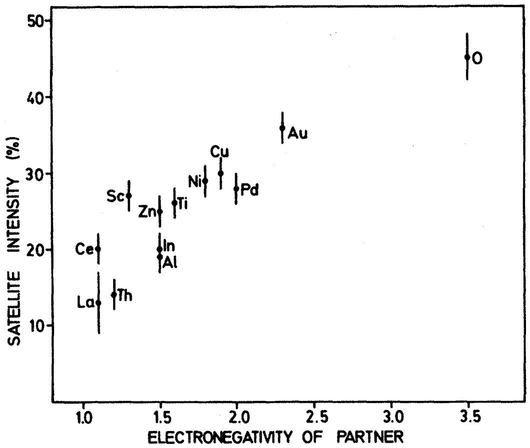

FIG. 10. Dependence of Ni $2p_{3/2}$ satellite intensity on electronegativity of partner element for 1:1 alloys. CeNi and ScNi do not follow the general trend (see Sec. IV A for a discussion).

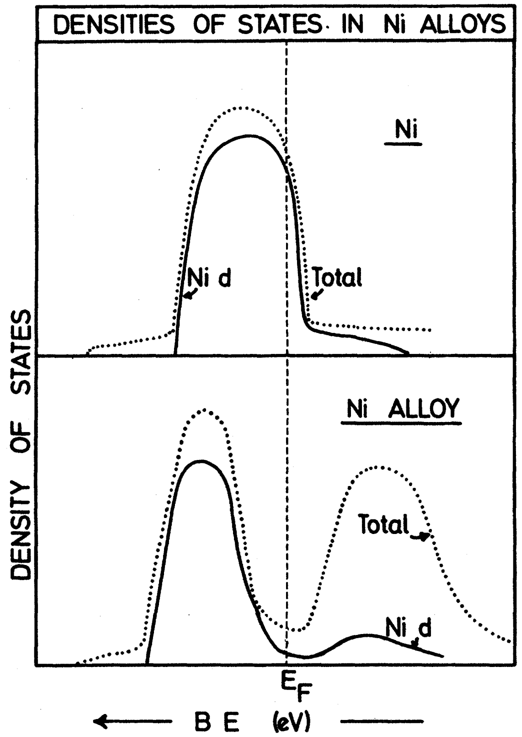

FIG. 11. Model of DOS's in Ni and Ni alloys with electropositive elements as proposed in paper I. In Ni there is a narrow d band superimposed on the flat and a much wider sp band which can be seen on both sides of the d band. The unoccupied part of the sp band also contains unoccupied d states above the main d band (Refs. 19, 23, and 59). In the alloy the d band is full, the DOS at E_F is reduced, and there are unoccupied Ni d states peaking at about the same position as the total DOS.

Although Feldkamp and Davis showed that it is possible to get resonant satellites in metals with a filled *d* band like Cu or Zn via holes in the 4*sp* band[32] we believe the XPS satellite intensity in alloys where the Ni *d* band is filled is too high to be explained by the *s*-*p* character alone. We believe that the satellite in these alloys arises mainly from the Ni *d* character in the "partner bands" which was indicated to be present by the calculations in paper I. As explained in Sec. I, the satellite contribution from this *d* character is weaker than that due to *d* holes in the Ni *d* band because the latter are always just above E_F. Ni *d* character which is strongly hybridized with other bands and shifted above E_F gives a weaker contribution to the satellite.

The important conclusion from our observations of satellite intensity as a function of stoichiometry is that filling of the Ni 3*d* band in alloys with electropositive elements does not imply charge transfer to the 3*d* orbitals. The observation of satellites, even in alloys such as Ce_7Ni_3 or Ta_2Ni implies the presence of *d* character in the unoccupied bands. In such alloys the Ni *d* bands have some character of the partner element, which allows them to become full without a large change in *d* count.

The second observation on satellite intensities was that there is a loose correlation between partner electronegativity and Ni satellite intensity. This might have been correlated with charge transfer, which is always considered to be larger with large electronegativity differences but as described in paper I and above, we have several reasons to reject the concept of large charge transfer to the Ni *d* levels. Basically our problem is that many of an element's properties scale loosely with electronegativity.[53,54] In general the electropositive element's, such as La, Th, Ce, and Sc have a large number of unfilled states. The calculations in paper I showed that the Ni *d* states mix with such unfilled bands. If the centroid of these bands is further above E_F, as in most electropositive elements, then this could "lift" the unoccupied Ni *d* character further above E_F, and thus decrease its contribution to the satellite. We can also suggest that the Ni satellite intensities in CeNi and ScNi, which lie somewhat above the general trend in Fig. 10, are raised by a high density of Sc and Ce states close to E_F. In CeNi these could be the Ce 4*f* states which are probably only partly occupied[55–58] giving rise to a very high DOS at E_F.

B. Effect of bandwidth *W*.

Bosch *et al.*[13] showed that reducing the bandwidth of the Ni *d* band by a factor of 20 led to a stronger satellite in XPS whose multiplet structure could be resolved. In the alloys investigated by us the bandwidth is reduced by a factor of 2 at the most, as can be seen from Tables IV and V of paper I. However, the satellite intensities are in all cases (except AuNi) smaller than in Ni. We conclude that the moderate reduction of the bandwidth does not have an appreciable influence on satellite intensity.

C. Multiplet splitting

In Ni_5Au_{95} (Ref. 13) it was found that the multiplet splitting of the $2p^5 3d^9$ final state is responsible for the different energy separations of the $2p_{1/2}$ and $2p_{3/2}$ satellites from the main lines, which in Ni metal are 4.6 and 5.8 eV, respectively. Also the difference in satellite intensity and shape between the $2p_{1/2}$ and $2p_{3/2}$ peaks is caused by multiplet splitting, which is smaller for the $2p_{1/2}$ level. We find in all alloys that the separation of the $2p_{1/2}$ satellite from the main line is smaller than that of the $2p_{3/2}$ satellite, their ratio being roughly the same as in Ni. We concur with the idea that the satellite consists of a multiplet whose splitting is roughly the same as in the Ni atom. The alloying changes the ability of the solid (or VB electrons) to screen the final state for both $2p^5 3d^9$ multiplets in the same way, leading to a similar shift of both satellites relative to the main lines.

In CuNi, PdNi, and AuNi the shape of the satellite seems to reflect the influence of the multiplet splitting, as the Ni $2p_{3/2}$ XPS spectrum from AuNi is intermediate between the Ni $2p_{3/2}$ XPS spectra from Ni and Ni_5Au_{95}.[13] In Ref. 13 it was pointed out that the satellite intensity is reduced if its separation, Δ, divided by the bandwidth *W* is small. The authors explained that the L_3 $2p^5 3d^9$ multiplet was spread out and that terms with smaller Δ were more strongly suppressed in Ni where *W* is about 4 eV. In Ni_5Au_{95} *W* is reduced to $\sim$200 meV and the low-Δ terms are observed. However, in AuNi, and in CuNi and PdNi as well, the width of the Ni *d* band as indicated by the XPS VB spectra (see paper I) is certainly not very different from Ni metal. The only explanation we can offer is that there are "clusters" with varying Ni concentrations, which accordingly should have different Ni 3*d* bandwidths. The Ni 2*p* XPS spectrum could then be understood as a superposition of a 2*p* spectrum corresponding to "Ni", and one more like the 2*p* spectrum from Ni_5Au_{95}. This explanation is not entirely satisfactory because only a small portion of Ni can be in Au-rich clusters.

D. Chemical shift

Tables III and IV give the BE's of the Ni $2p$ levels, while Table V gives the BE's of other Ni core levels. The last columns give the chemical shifts. The chemical shifts in Ni intermetallic compounds are smaller than those from Pd intermetallic compounds; shifts larger than 0.5 eV are very rare. It has been shown that the chemical shifts of XPS core lines in alloys can be related to the heat of solution of a $Z+1$ atom in the matrix.[21,22,41,42] Thus in the case of Ni and Pd alloys the shifts are determined primarily by the alloying properties of Cu and Ag. A full discussion of this effect is beyond the scope of this paper and will be published separately.[50]

V. CONCLUSIONS

In this paper we have investigated dependence of the Ni core-level XPS satellites on chemical environment. The results from alloys with electropositive metals, M, are interpreted in terms of a model where admixture of M orbital character to the Ni d states is more important for band filling than charge transfer. In such alloys there is an initial sharp decrease in satellite intensity as the Ni is diluted and the Ni d band is filled, in accordance with the suggestion[15] that the satellite intensity may give information on the number of holes in the Ni d band. However, the satellite intensities do not decrease to zero because the unoccupied states still have a minor contribution of Ni d character in agreement with suggestions resulting from theoretical investigations.[59] For the satellite intensity the *energy distribution* of this d character has importance at least comparable to the importance of the *quantity* of unoccupied d character.

These results suggest several future lines of investigation. Calculations of the Ni core-level satellite intensities in a formalism like that of Feldkamp and Davis, using the band structure of Ni alloys would be of great interest to define more clearly the role of the energy of the unoccupied states. Ideally such calculations should include the $2p^5 3d^9$ multiplet splitting. It would also be interesting to compare the changes in core-level satellite intensity with changes in the intensity of the VB satellite in Fano resonance.

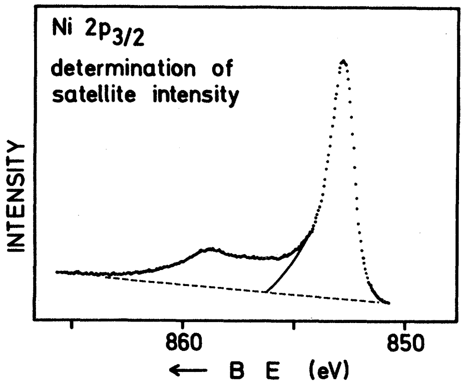

FIG. 12. Determination of satellite intensity for the example fo the $2p_{3/2}$ level of Ni.

ACKNOWLEDGMENTS

We are grateful to Professor M. Campagna for his continued support and encouragement of this work. We also thank A. Bringer, J. Fink, W. Gudat, O. Gunnarsson, J. Harris, B. Johansson, R. O. Jones, G. A. Sawatzky, and K. Schönhammer for discussions. Able technical assistance was provided by M. Beyss, H. Gier, J. Keppels, U. Mambor, J.-M. Welter, and E. M. Wurtz.

APPENDIX: DETERMINATION OF SATELLITE INTENSITY

Satellite intensities were determined graphically on the plots which were also used for drawing the figures. We assumed a linearly increasing background, indicated by the dashed line in Fig. 12. ELS measurements in reflection on some Ni alloys showed that this was a good approximation. We then extrapolated the high-BE side of the main line down to the background line (full line in Fig. 12). The extrapolation is to some extent arbitrary, but as long as it is done consistently the results are reproducible and can be compared to each other. The areas of main peak and satellite were then determined, and the satellite intensity was calculated using the formula

$$I_{\text{rel sat}} = \frac{n_{\text{sat}}}{(n_{\text{sat}} + n_{\text{ml}})} ,$$

where n_{sat} and n_{ml} are the areas of satellite and main line, respectively.

[*] Present address: Bell Laboratories, Murray Hill, New Jersey 07974.

[†] Present address: Institute for Low Temperature and Structure Research, Polish Academy of the Sciences, P. O. Box 937, 50-950 Wroclaw, Poland.

[1] J. C. Fuggle, F. U. Hillebrecht, R. Zeller, Z. Zołnierek, P. Bennett, and Ch. Freiburg, preceding paper, Phys. Rev. B 27, 2145 (1983).

[2] R. Manne and T. Åberg, Chem. Phys. Lett. 7(2), 282 (1970).

[3] T. A. Carlson, M. O. Krause, and W. E. Moddeman, J. Phys. (Paris) 32, C4-76 (1971).

[4] G. A. Vernon, G. Stucky, and T. A. Carlson, Inorg. Chem. 15, 278 (1976).

[5] K. Siegbahn, C. Nordling, G. Johannsson, J. Hedman, P. F. Hedin, K. Hamrin, U. Gelius, T. Bergmark, L. O. Werme, R. Manne, and Y. Baer, *ESCA Applied to Free Molecules* (North-Holland, Amsterdam, 1971).

[6] P. S. Bagus, Phys. Rev. 139, A619 (1965).

[7] A. Rosencwaig, G. K. Wertheim, and H. J. Guggenheim, Phys. Rev. Lett. 27, 479 (1971).

[8] N. J. Shevchik, Phys. Rev. Lett. 33, 1336 (1974); Phys. Status Solidi 59, 87 (1973).

[9] S. Hüfner and G. K. Wertheim, Phys. Lett. 51A, 299, 301 (1975).

[10] S. P. Kowalczyk, Ph.D. thesis, University of California, Berkeley, 1976 (unpublished).

[11] S. P. Kowalczyk, G. Apai, G. Kaindl, F. R. McFeely, L. Ley, and D. A. Shirley, Solid State Commun. 25, 847 (1978).

[12] P. T. Andrews, T. Collins, C. E. Johnson, and P. Weightman, J. Electron Spectrosc. and Relat. Phenom. 15, 39 (1979).

[13] A. Bosch, H. Veil, G. A. Sawatzky, and N. Mårtensson, Solid State Commun. 41, 355 (1982).

[14] N. Mårtensson and B. Johannsson, Phys. Rev. Lett. 45, 482 (1980).

[15] J. C. Fuggle and Z. Zolnierek, Solid State Commun. 38, 799 (1981).

[16] N. F. Mott, Adv. Phys. 13, 325 (1964), and references therein.

[17] H. Danan, A. Herr, and A. J. P. Meyer, J. Appl. Phys. 39, 669 (1968), and references therein.

[18] L. Hodges, H. Ehrenreich, and N. D. Lang, Phys. Rev. 152, 505 (1966).

[19] M. C. Munoz, P. J. Durham, and B. L. Gyorffy, J. Phys. F (in press).

[20] W. L. Jolly, in *Electron Spectroscopy,* edited by D. A. Shirley (North-Holland, Amsterdam, 1972), p. 629.

[21] N. Mårtensson and B. Johannsson, Solid State Commun. 32, 791 (1979).

[22] B. Johansson and N. Mårtensson, Phys. Rev. B 21, 4427 (1980), and references therein.

[23] See Ref. 5 in A. R. Williams and N. O. Lang, Phys. Rev. Lett. 40, 954 (1978).

[24] P. Steiner, H. Höchst, W. Steffen, and S. Hüfner, Z. Phys. B 38, 191 (1980).

[25] H. Höchst, P. Steiner, and S. Hüfner, Z. Phys. B 38, 201 (1980).

[26] A. Kotani and Y. Toyozawa, J. Phys. Soc. Jpn. 35, 1073,1082 (1973); 37, 912 (1974).

[27] A. Kotani, J. Phys. Soc. Jpn. 46, 488 (1979).

[28] K. Schönhammer and O. Gunnarsson, Solid State Commun. 23, 691 (1977); 26, 147,399 (1978); Z. Phys. B 30, 297 (1978).

[29] O. Gunnarsson and K. Schönhammer, Phys. Rev. Lett. 41, 1608 (1978).

[30] J. C. Fuggle, E. Umbach, D. Menzel, K. Wandelt, and C. R. Brundle, Solid State Commun. 27, 65 (1978).

[31] D. R. Penn, Phys. Rev. Lett. 42, 921 (1979).

[32] L. A. Feldkamp and L. C. Davis, J. Appl. Phys. 50, 1944 (1979); Phys. Rev. B 22, 3644 (1980); Phys. Rev. Lett. 44, 673 (1980).

[33] A. Liebsch, Phys. Rev. Lett. 43, 1431 (1979); Phys. Rev. B 23, 5203 (1981).

[34] J. C. Fuggle, M. Campagna, Z. Zołnierek, R. Lässer, and A. Platau, Phys. Rev. Lett. 45, 1597 (1980).

[35] J. C. Fuggle, in *Inner Shell and X-Ray Physics of Atoms and Solids,* edited by D. J. Fabian, H. Kleinpoppen, and L. M. Watson (Plenum, New York, 1981), pp. 485–488.

[36] L. Ley, S. P. Kowalczyk, F. R. McFeely, R. A. Pollak, and D. A. Shirley, Phys. Rev. B 8, 2392 (1973).

[37] J. Tersoff, L. M. Falicov, and D. R. Penn, Solid State Commun. 32, 1045 (1979).

[38] G. D. Mahan, Phys. Rev. 163, 612 (1967); P. Nozières and C. T. de Dominicis, Phys. Rev. 178, 1097 (1969).

[39] S. Doniach and M. Šunjić, J. Phys. C 3, 285 (1970).

[40] K. Siegbahn, C. Nordling, A. Fahlman, R. Nordberg, K. Hamerin, J. Hedman, G. Johansson, T. Bergmark, S.-E. Karlsson, I. Lindgren, and B. Lindberg, *Electron Spectroscopy for Chemical Analysis—Atomic, Molecular, and Solid State Structure Studies by Means of Electron Spectroscopy* (Almqvist and Wiksells, Stockholm, 1967); Nova Acta Regiae Soc. Sci. Ups. Ser. IV, 20 (1967).

[41] P. Steiner, S. Hüfner, N. Mårtensson, and B. Johannsson, Solid State Commun. 37, 73 (1981).

[42] P. Steiner and S. Hüfner, Solid State Commun. 37, 79 (1981).

[43] S. Hüfner, G. K. Wertheim, and J. H. Wernick, Solid State Commun. 17, 417 (1975).

[44] D. Chandesris, G. Krill, G. Maire, J. Lecante, and Y. Petroff, Solid State Commun. 37, 187 (1981).

[45] J. Daniels, Z. Phys. 227, 234 (1969).

[46] P. H. Staib and K. Ulmer, Z. Phys. 219, 381 (1969).

[47] N. Mårtensson, R. Nyholm, and B. Johannsson (unpublished).

[48] For a review, see, e.g., H. Raether, *Excitation of Plasmons and Interband Transitions by Electrons,* Vol. 88 of *Springer Tracts in Modern Physics* (Springer, Berlin, 1980).

[49] A. R. Miedema, P. F. de Châtel, and F. R. de Boer, Physica 100B, 1 (1980); quoted values taken from Table V b.

[50] F. U. Hillebrecht and J. C. Fuggle (unpublished).

[51] W. Gordy and W. J. O. Thomas, J. Chem. Phys. 24, 439 (1955).

[52] J. Brunner, private communication.

[53] M. C. Day and J. Selbin, *Theoretical Inorganic Chemistry* (Reinhold, New York, 1965), pp. 111ff.

[54] L. H. Bennett and R. E. Watson, in *Theory of Alloy Phase Formation,* edited by L. H. Bennett (The Metallurgical Society of AIME, New York, 1980), pp. 390–423 (especially p. 396ff).

[55] G. Krill, J. P. Kappler, A. Meyer, L. Abadli, and M. F. Ravet, J. Phys. F 11, 1713 (1981).

[56] See, e.g., *Proceedings of the International Conference on Intermediate Valence Compounds, Santa Barbara, 1981,* edited by L. M. Falicov, W. Hanke, and M. B. Maple (North-Holland, Amsterdam, 1981).

[57] *Handbook on the Physics and Chemistry of Rare Earths,* edited by K. A. Gschneidner and L. Eyring (North-Holland, Amsterdam, 1979), Vol. I. Chap. IV, p. 337.

[58] J. C. Fuggle, F. U. Hillebrecht, Z. Zołnierek, R. Lässer, and Ch. Freiburg (unpublished).

[59] H. Akai, J. Phys. Soc. Jpn. (in press).